

HW2-Explain asymmetric miscibility gap

Modeling of Miscibility Gap 1

Ref. Young-Bae Kang, Arthur D. Pelton
"The shape of **liquid miscibility gaps** and short range order"

Typical Modeling Equations

$$G = X_A G_A^o + X_B G_B^o + RT(X_A \ln X_A + X_B \ln X_B) + G^E$$

with the molar Gibbs energy given as:

$$G^E = H^E - TS^E = \alpha_{AB} X_A X_B$$

where X_i and G_i^o are the molar fraction and standard molar Gibbs energy of component i , and R is the ideal gas constant.

The configurational entropy $-R(X_A \ln X_A + X_B \ln X_B)$ is obtained from the Bragg-Williams assumption of random mixing of A and B on a quasilattice. If the parameter α_{AB} is positive, a miscibility gap results.

Using Bragg-Williams empirical expansion

In order to fit experimental phase equilibrium and thermodynamic data and develop databases of model parameters, following expansion is used.

$$\alpha_{AB} = L_{AB}^0 + L_{AB}^1(X_B - X_A) + L_{AB}^2(X_B - X_A)^2 + \dots$$

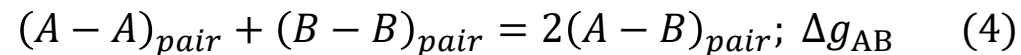
where the L_{AB}^k are empirical model parameters which may be functions of T .

Fit Result : To reproduce adequately experimental binary miscibility gaps, ***several empirical terms are required in equation above***. If only two or three temperature independent parameters are used, ***the resultant calculated gaps are usually significantly higher and more rounded than experimental gaps which tend to be "flatter"***.

Fit Resultant is posted as Figure 1,2

Modified quasi-chemical model (MQM) in the nearest-neighbor pair approximation

Consider a solution of atoms or molecules A and B which are distributed over the sites of quasi-lattice. A first-nearest-neighbor pair exchange reaction can be written:



If the Gibbs energy change Δg_{AB} of this reaction is positive, then (A-A) and (B-B) pairs are favored over (A-B) pairs. In the random mixing Bragg-Williams approximation, the probabilities of (A-A), (B-B) and (A-B) pairs are always X_A^2 , X_B^2 , and $2X_A X_B$ respectively. Hence, the system can only reduce the number of energetically unfavorable (A-B) pairs by separating into two immiscible phases.

In reality, however, clustering of A and B can occur within a single-phase solution, thereby permitting an increase in the number of favorable (A-A) and (B-B) pairs without separation into two phases. Such clustering will be most pronounced, and have the greatest effect in lowering the Gibbs energy, in the central composition region where $X_A \approx X_B$. In the dilute terminal composition regions, the configurational entropy terms predominate and so the solution tends toward random mixing. As a result, short-range-order(SRO) has the largest effect on lowering the miscibility gap in the central composition region, thereby producing the observed "flattened" shape.

MQM modeling equations

Let Z be the nearest-neighbor coordination number. Then, for one mole of solution:

$$ZX_A = 2n_{AA} + n_{AB} \quad (5)$$

$$ZX_B = 2n_{BB} + n_{AB} \quad (6)$$

where n_{AA} , n_{BB} and n_{AB} are the numbers of moles of pairs in one mole of solution. Pair fractions X_{ij} are defined as:

$$X_{ij} = \frac{n_{ij}}{n_{AA} + n_{BB} + n_{AB}} \quad (7)$$

The molar Gibbs energy is assumed to be given by:

$$g = (X_A g_A^o + X_B g_B^o) + \left(\frac{n_{AB}}{2}\right) \Delta g_{AB} - T \Delta S^{config} \quad (8)$$

The configurational entropy ΔS^{config} is given by randomly distributing the first-neighbor pairs over "pair positions". In three dimensions the exact mathematical expression is unknown. The following approximate expression is obtained:

$$\Delta S^{config} = -R(X_A \ln X_A + X_B \ln X_B) - R \left[n_{AA} \ln \left(\frac{X_{AA}}{X_A^2} \right) + n_{BB} \ln \left(\frac{X_{BB}}{X_B^2} \right) + n_{AB} \ln \left(\frac{X_{AB}}{2X_A X_B} \right) \right] \quad (9)$$

MQM modeling equations

Minimizing the Gibbs energy subject to the constraints of equations (5) and (6) yields the following “quasi-chemical equilibrium constant” for reaction (4):

$$\frac{X_{AB}^2}{X_{AA}X_{BB}} = 4 \exp\left(-\frac{\Delta g_{AB}}{RT}\right) \quad (10)$$

At a given composition, and for a given value of Δg_{AB} , equations (5), (6), and (10) can be solved to give X_{ij} which can then be substituted back into equations (7)-(9). When $\Delta g_{AB} = 0$, the solution is a random ideal solution. As Δg_{AB} becomes progressively more positive, reaction (4) is displaced progressively to the left and the degree of short-range-order increases.

For purposes of optimization, Δg_{AB} may be explained as a polynomial in mole fractions:

$$l_{AB}^0 + l_{AB}^1(X_B - X_A) + l_{AB}^2(X_B - X_A)^2 + \dots \quad (11)$$

where l_{AB}^k are adjustable model parameters. When Δg_{AB} is small, it follows from equation (10) that the pair fractions are close to their values in a randomly distributed solution ($X_{AA} = X_A^2$, $X_{BB} = X_B^2$, $X_{AB} = 2X_A X_B$). Hence the configurational entropy is close to the ideal (Bragg-Williams) entropy, and $n_{AB} \approx 2X_A X_B \left(\frac{Z}{2}\right)$, where $\left(\frac{Z}{2}\right)$ is the total number of pairs in a mole of solution. The molar Gibbs energy expression from equation (8) is then approximately the same as equations (1) and (2) with $\alpha \approx \Delta g_{AB} \left(\frac{Z}{2}\right)$ and with all parameters $L_{AB}^k \approx l_{AB}^k (Z/2)$.

MQM modeling fit

Equation (9) for the entropy can be shown to be exact only for a one-dimensional lattice ($Z = 2$). In three dimensions the equation is only approximate since no exact solution of the three dimensional Ising model is known. The error introduced by this approximation can be offset through the choice of somewhat non-physical values of Z . From our experience in applying the MQM to many liquid metallic solutions, we have found that a value of approximately $Z = 6$ yields the best results, although the calculations are not highly sensitive to this parameter.

Fitting result: Figure 1~2

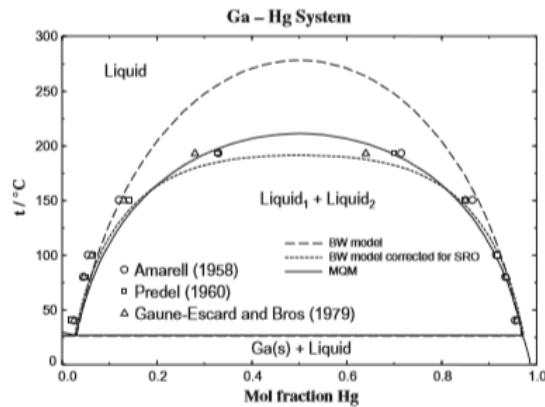


FIGURE 1. Ga-Hg phase diagram calculated with different models and experimental data points (see Refs. [1-3]).

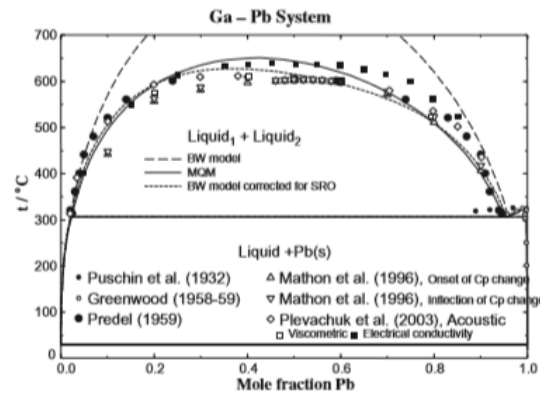


FIGURE 2. Ga-Pb phase diagram calculated with different models and experimental data points (see Refs. [4-8]).

MQM modeling fit result- (Ga+Hg) system

The miscibility gap in the (Ga+Hg) system with the MQM with one temperature-independent parameter, , $\Delta g_{GaHg} \left(\frac{Z}{2} \right) = 9790 J \cdot mol^{-1}$, selected so as to reproduce the measured monotectic temperature and compositions.

It can be seen in figure 1 that the experimental miscibility gap is reproduced very closely at all temperatures and compositions.

Furthermore, as seen in figure 3, the measured excess enthalpy is also reproduced very closely.

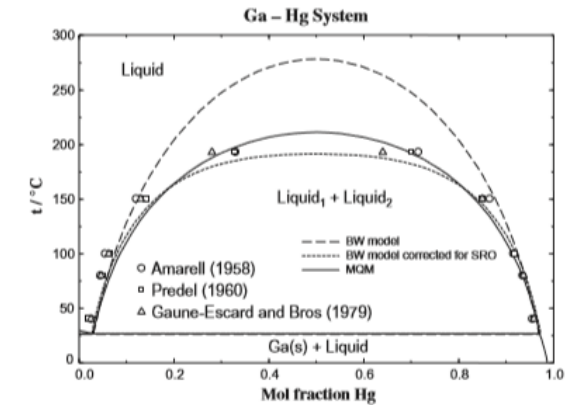


FIGURE 1. Ga-Hg phase diagram calculated with different models and experimental data points (see Refs. [1-3]).

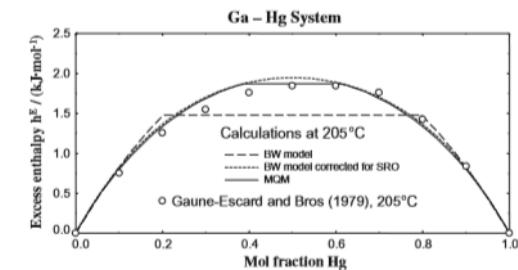


FIGURE 3. Excess enthalpies in Ga-Hg liquid solutions calculated with different models and experimental data points (see Ref. [3]).

MQM modeling fit result- (Ga+Pb) system

For (Ga+Pb) system, two temperature-independent parameters were used. Again, the experimental miscibility gap and excess enthalpy are reproduced very well.

It can be seen in table 1 that the numeric values of the MQM parameters are very similar to those used in the Bragg-Williams model.

Note that the data for h^E are closely reproduced even though the model parameters are temperature-independent, thereby showing that the entropy is well represented by the configurational entropy expression in equation (9); non-configurational excess entropy terms are not required.

TABLE 1
Model parameters used in calculations ($\text{J} \cdot \text{mol}^{-1}$) (BW = Bragg-Williams; MQM = modified quasi-chemical model).

Z = 6		
Ga-Hg	BW	$\alpha = 9163$
	MQM	$\Delta g(z/2) = 9790$
Ga-Pb	BW	$\alpha = 17950 + 1506(X_{\text{Ga}} - X_{\text{Pb}})$
	MQM	$\Delta g(z/2) = 18263 + 1506(X_{\text{Ga}} - X_{\text{Pb}})$
Ga-Tl	BW	$\alpha = 16945 + 1506(X_{\text{Ga}} - X_{\text{Tl}})$
	MQM	$\Delta g(z/2) = 17573 + 1506(X_{\text{Ga}} - X_{\text{Tl}})$
Al-In	MQM	$\Delta g(z/2) = 23849 + 2510(X_{\text{Al}} - X_{\text{In}})$

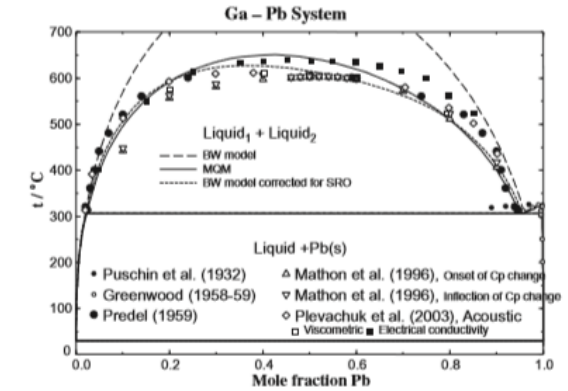


FIGURE 2. Ga-Pb phase diagram calculated with different models and experimental data points (see Refs. [4-8]).

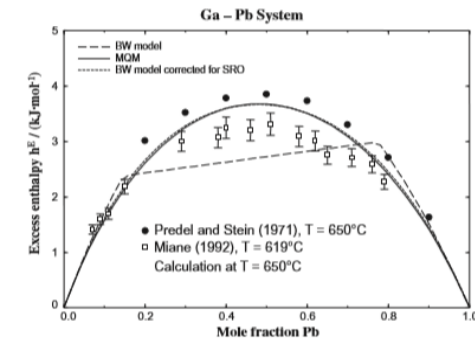


FIGURE 4. Excess enthalpies in Ga-Pb liquid solutions calculated with different models and experimental data points (see Ref. [9,10]).

MQM modeling fit conclusion

Most systems with liquid miscibility gaps, only limited data are available. Generally, the boundaries of the gaps have been measured only near the monotectic temperatures, not near the consolute temperatures, and data for the excess enthalpy are lacking. In such cases if the empirical MQM parameters are optimized based only on the measured compositions of the boundaries of the miscibility gap at lower temperatures, the gap boundaries at higher temperatures and the excess enthalpy will be predicted by the MQM with much better accuracy than is the case with the Bragg-Williams model.

Modeling of Miscibility Gap 1

Ref. H.K. Hardy

"A 'Sub-Regular' Solution model and its application to some binary alloy systems"

Sub-Regular Solutions

The excess molar heat of solution of a binary solid solution is given by

$$\Delta H = \frac{1}{2}ZN(2V_{XY} - (V_{XX} + V_{YY}))xy = Axy$$

where Z is the coordination number, N is the Avogadro's number, V_{XY} , V_{XX} , and V_{YY} are the interaction energies, and x and y are the atomic fractions of X and Y components.

The next simple assumption is to make A a rectilinear function of composition so that

$$\Delta H = (A_1x + A_2y)xy = A_1x^2y + A_2xy^2$$

and the model may logically be termed "sub-regular".

Sub-Regular Solutions

The free energy per mole is given by

$$F = x\mu_X^0 + y\mu_Y^0 + A_1x^2y + A_2xy^2 + RT(x\ln x + y\ln y) \quad (5)$$

so that the chemical potentials are

$$\begin{aligned}\mu_X &= \mu_X^0 + RT\ln x + y^2(2A_1 - A_2) + y^2(2A_2 - 2A_1) \\ \mu_Y &= \mu_Y^0 + RT\ln y + x^2(2A_2 - A_1) + x^2(2A_1 - 2A_2)\end{aligned} \quad (6)$$

Differentiation gives

$$\begin{aligned}\frac{\partial \mu_X}{\partial x} &= \frac{RT}{x} + 2A_1y(1 - 3x) + 2A_2y(1 - 3y) \\ \frac{\partial^2 \mu_X}{\partial x^2} &= -\frac{RT}{x^2} + 2A_1(6x - 4) + 2A_2(5 - 6x) \\ \frac{\partial \mu_Y}{\partial y} &= \frac{RT}{y} + 2A_1x(1 - 3x) + 2A_2x(1 - 3y) \\ \frac{\partial^2 \mu_X}{\partial x^2} &= -\frac{RT}{y^2} + 2A_1(5 - 6y) + 2A_2(6y - 4)\end{aligned} \quad (7a)\sim(7d)$$

Sub-Regular Solutions

The spinodal curve is obtained by equating equations (7a) or (7c) to zero so that

$$RT = 2x^2y(2A_1 - A_2) + 2xy^2(2A_2 - A_1)$$

Equations (7b) and (7d) are also zero at the critical point for phase separation, subtracting equation (7d) from (7b) and re-arranging gives

$$RT(x - y) = 6x^2y^2(A_1 - A_2)$$

Solving between equations (8) and (9) gives A_1 and A_2 at the critical point and

$$A_1 = \frac{RT}{6x_e^2y_e^2}(-9x_e^2 + 10x_e - 2)$$
$$A_2 = \frac{RT}{6x_e^2y_e^2}(-9y_e^2 + 10y_e - 2)$$

Sub-Regular Solutions

$A_1 = A_2 = 2RT_e$ when $x_e = 0.5$ and the equations reduce to these for a regular solution with a symmetrical solubility curve. The difference between A_1 and A_2 increases as x_e deviates from the equiatomic composition. A_1 is zero when $x_e = 0.26$ and 0.85 . Solubility curves which are very strongly asymmetrical require both A_1 and A_2 to be negative.

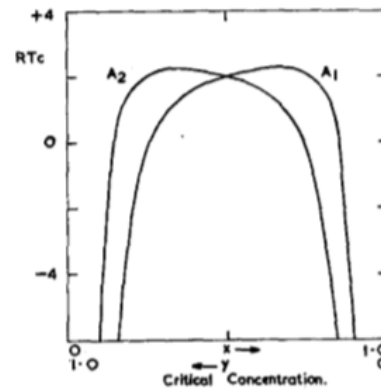


FIGURE 1. Values of A_1 and A_2 corresponding to different critical concentrations.

Sub-Regular Solutions

The solid solubility boundaries are defined by the conditions

$$\mu_X(1) = \mu_X(2) \quad (11a)$$

$$\mu_Y(1) = \mu_Y(2) \quad (11b)$$

making the chemical potential of each component equal in the equilibrium co-existing phases. The values of A_1 and A_2 in equation (6) can thus be calculated from the solubility data at any temperature, since the terms in μ^0 cancel in equations (11), as long as the two terminal solid solutions have the same lattice structure. Only systems in which it is hypothetically possible to have unlimited solubility above a critical temperature (which may be above the melting point) are dealt with in the present work.

Sub-Regular Solutions

Subtracting equations (11a) and (11b), inserting the values from equations (6) and rearranging leads to

$$RT \ln \left(\frac{x_1}{x_2} \right) - RT \ln \left(\frac{y_1}{y_2} \right) - A_1(x_1 - x_2)(3x_1 + 3x_2 - 2) + A_2(y_1 - y_2)(3y_1 + 3y_2 - 2) = 0$$

where x_1, x_2, y_1, y_2 are the atomic fractions at the solubility curves. This may be compared with the equation for the solubility curve of a regular solution which is

$$RT \ln \left(\frac{x_1}{x_2} \right) - A(x_1 - x_2) = 0$$

Multiplying equation (11a) by $(x_1 + x_2)$ and equation (11b) by $(y_1 + y_2)$, adding and simplifying gives

$$\begin{aligned} \phi &\equiv (x_1 + x_2)RT \ln \left(\frac{x_1}{x_2} \right) + (y_1 + y_2)RT \ln \left(\frac{y_1}{y_2} \right) \\ &= -(A_1 - A_2)(x_1 - x_2)^3 \end{aligned}$$

In which both sides are zero for a regular solution. When the left-hand side is plotted against $(x_1 - x_2)^3$ a straight line passing through the origin at $T = T_e$ will be obtained as long as $A_1 - A_2$ is independent of temperature.

Sub-Regular Solutions – Stepping Further

The interpretation of A_1 and A_2 is not limited to heats of solution but they can also be identified with a free energy of solution. They will then be temperature dependent, but this in no way influences the previous analysis which has, in effect, been carried out at constant temperature. The entropy and heat of solution must of course be obtained by differentiation of equation (5) and the latter is no longer given by equation (2).